A Framework for Representation and Visualization of 3D Shape Variability of Organs in an Interactive Anatomical Atlas

S. Hacker; H. Handels
Department of Medical Informatics, University Medical Center Hamburg-Eppendorf,
Hamburg, Germany

Keywords
3D-visualization, anatomical atlas, medial representation, medical education, shape modeling, statistical shape models

Summary

Objectives: Computerized anatomical 3D atlases allow interactive exploration of the human anatomy and make it easy for the user to comprehend complex 3D structures and spatial interrelationships among organs. Besides the anatomy of one reference body inter-individual shape variations of organs in a population are of interest as well. In this paper, a new framework for representation and visualization of 3D shape variability of anatomical objects within an interactive 3D atlas is presented.

Methods: In the VOXEL-MAN atlases realistic 3D visualizations of organs in high quality are generated for educational purposes using volume-based object representations. We extended the volume-based representation of organs to enable the 3D visualization of organs' shape variability in the atlas. Therefore, the volume-based representation of the inner organs in the atlas is combined with a medial representation of organs of a population creating a compact description of shape variability.

Results: With the framework developed different shape variations of an organ can be visualized within the context of a volume-based anatomical model. Using shape models of the kidney and the breathing lung as examples we demonstrate new possibilities such an approach offers for medical education. Furthermore, attributes like gender, age or pathology as well as shape attributes are assigned to each shape variant which can be used for selecting specific organs of the population.

Conclusions: The inclusion of anatomical variability in a 3D interactive atlas presents considerable challenges, since such a system offers the chance to explore how anatomical structures vary in large populations, across age, gender and races, and in different disease states. The framework presented is a basis for the development of specialized variability atlases that focus e.g. on specific regions of the human body, groups of organs or specific topics of interest.

Correspondence to:
Prof. Dr. Heinz Handels
Department of Medical Informatics
University Medical Center Hamburg-Eppendorf
Martinistr. 52
20246 Hamburg
Germany
E-mail: h.handels@uke.uni-hamburg.de

Methods Inf Med 2009; 48: 272–281
doi: 10.3414/ME0551
received: March 7, 2008
accepted: July 9, 2008
prepublished: March 31, 2009

1. Introduction

Computer-based 3D atlases of the human body have experienced a remarkable change during the last two decades. They have evolved from simple anatomy atlases that were suited only for the interested amateur to highly professional tools for medical education and practice. Nowadays they are not only a valuable tool for learning and teaching anatomy but also a reference used e.g. by health professionals. 3D models of the human body on which such atlases are based are typically constructed from 3D image data generated e.g. by computer tomography (CT) or magnetic resonance imaging (MRI). With the Visible Human project [1, 2] high-resolution cross-sectional photographic images became available which provide a basis for the generation of 3D models with a high degree of detail. Similar projects with photographic data sets of even higher resolutions followed, as e.g. the Chinese Visible Human [3] or the Visible Korean Human data set [4]. Using these data sets a variety of research projects for the development of 3D models and digital atlases of the human body came to be developed.

Computerized anatomical atlases based on high-quality 3D models are a useful addition to printed anatomy atlases. In contrast to static knowledge representation in textbooks, they allow interactive exploration of the human anatomy and make it easier for the user to understand complex 3D structures and spatial interrelationships among organs. Besides the high quality and flexibility computer-based atlases have reached these days, they still have their limitations. In most cases 3D atlases are derived from a single individual, or a very small number of subjects, and are not representative of the human anatomy in general [5, 6]. They do not contain any information about how and to what extent anatomical structures vary between different people. Yet, in reality there are considerable differences regarding the shape and size of anatomical objects, which is partly due to natural variability, but may also be affected by factors like age, gender, ethnic background, diseases or habits. The investigation of anatomical shapes and their variability can improve the understanding of processes behind growth, ageing or diseases and support medical diagnostics and therapy. Thus, the inclusion of variability into an anatomical atlas would be a great advancement and would be useful not only for students learning anatomy but also for medical experts. This paper presents a new approach representing inter- and intra-individual shape variability of anatomical objects in space and time within an interactive 3D atlas. The concept is explained and the possibilities of this approach are shown using shape models of the kidney and the lung as examples.

Size and shape of anatomical structures and their variability have always played an important role in medical education and research. Knowledge about variability in anatomy has traditionally been transmitted by sets of illustrative examples, as in collections of pictures or preparations. Most of today's digitized atlases which deal with anatomical variability use a similar approach like conventional atlas books, in that they usually show a number of normal and abnormal variations in schematic or photographic pictures accompanied by descriptive text. An example for such an approach is the "Multimedia Human Anatomic Variation Atlas" by Bergman et al. [7].

The integration of anatomical variability across whole populations in a 3D atlas still remains a challenging problem which is not yet generally solved. So far, most progress has been achieved for population-based atlases of the brain [8]. Here large sets of images are mapped into a common coordinate system using registration algorithms. The resulting deformation fields can then be used to create probability maps which retain information on anatomical variability. Such an approach is employed in an ongoing large-scale project of the International Consortium for Brain Mapping (ICBM) in which a probabilistic atlas of the human brain is being developed based on a large sample of normal individuals [9]. Also, a number of disease-specific atlases of the human brain have been developed using registration and warping algorithms which focus on revealing structural changes due to neurological diseases such as autism, schizophrenia, or Alzheimer's disease [8, 10].

Variability atlases based on deformation fields of large populations are powerful research tools with a wide range of clinical and scientific applications. They contain information about positional variability at every voxel related to a common reference space and allow a comparative examination of the anatomy of a high number of individuals. However, as anatomical structures differ not only in shape and size but also in relative orientation and position to each other, different kinds of information are superimposed in the deformation fields. This can make it difficult to interpret the resultant probability maps.

For an atlas which is focused on shape variability of individual anatomical structures rather than positional variability related to a global reference coordinate system, an organ-based approach using shape descriptors is suitable. For modeling and analysis of organ shapes a great number of shape descriptors and shape models have been proposed over the years like e.g. point distribution models [11], medial axes [12, 13], Fourier descriptors [14, 15], spherical harmonic functions [16], and active shape models [17]. Such methods have been applied mainly for model-based segmentation and classification of organ shapes. In our approach 3D shape models for representation of geometric variability are used in an interactive anatomical atlas as a new tool in medical education.

To demonstrate the possibility and functionality of an interactive anatomical atlas visualizing 3D shape variations of organs we have generated statistical models of the left kidney and of the breathing lung as examples. The kidney model is based on a population of 48 kidneys and captures inter-individual variability. The lung model encodes intra-individual shape variation during the breathing cycle based on 4D CT image data acquired during free breathing. Here, a 4D dataset consists of ten 3D image datasets measured in different breathing phases. Hence, the segmented lungs of the 4D image data reflect intra-individual respiratory shape variations of the lungs, which are modeled by m-reps.

2. Material and Methods

The basis of this work is the VOXEL-MAN atlas of the inner organs [5] which was developed at our department. It has been created from the photographic cross-sections and CT data of the Visible Human Male [1, 2]. A 3D model of the torso of the Visible Human has been built using color-space segmentation and a matched volume visualization technique [18]. The model is characterized by a high level of detail and contains more than 650 3D anatomical structures. The segmented anatomical objects are textured with their original colors and their surfaces are visualized with subvoxel resolution. That way a nearly photo-realistic quality is achieved (▶Fig. 1). Since it is a volume-based model of the human body, external surfaces of an organ can be viewed as well as interior views can be generated using cutting planes. Non-segmentable objects, like nerves and small blood vessels, were modeled artificially on the basis of landmarks present in the image volume.

The spatial model is connected to a symbolic model which contains descriptive information about their anatomical structures. Interrelations between objects are described via a semantic network [19, 20]. Examples of relations are "is part of", "has part" or "is branching from". The integrated knowledge base system allows a versatile object-based interaction with the spatial model, e.g. the 3D model can be interrogated or disassembled by addressing names of organs.

The volume-based model allows a highly realistic visualization of anatomical structures, but it is not suitable for an efficient representation of anatomical variability based on larger populations. Therefore, we extended the VOXEL-MAN system by a shape description that is connected to the volume model. The choice of shape representation depends strongly on the type of application at hand. For modeling anatomical shapes and their variability in an interactive 3D atlas we have chosen to use the medial model representation called "m-rep" [21, 22]. We have chosen the m-rep description for the representation of shape variability within the presented framework for the following reasons:

- M-reps offer a compact description of shape. They represent characteristic shape properties in an efficient way using a limited number of parameters (compared e.g. to the high-dimensional feature space of a 3D deformation field).
- Geometric correspondence of shape variants can be established not only between surface points but also between volume points. This is an important property for our purpose as the shape description is to combine with a volume-based model.

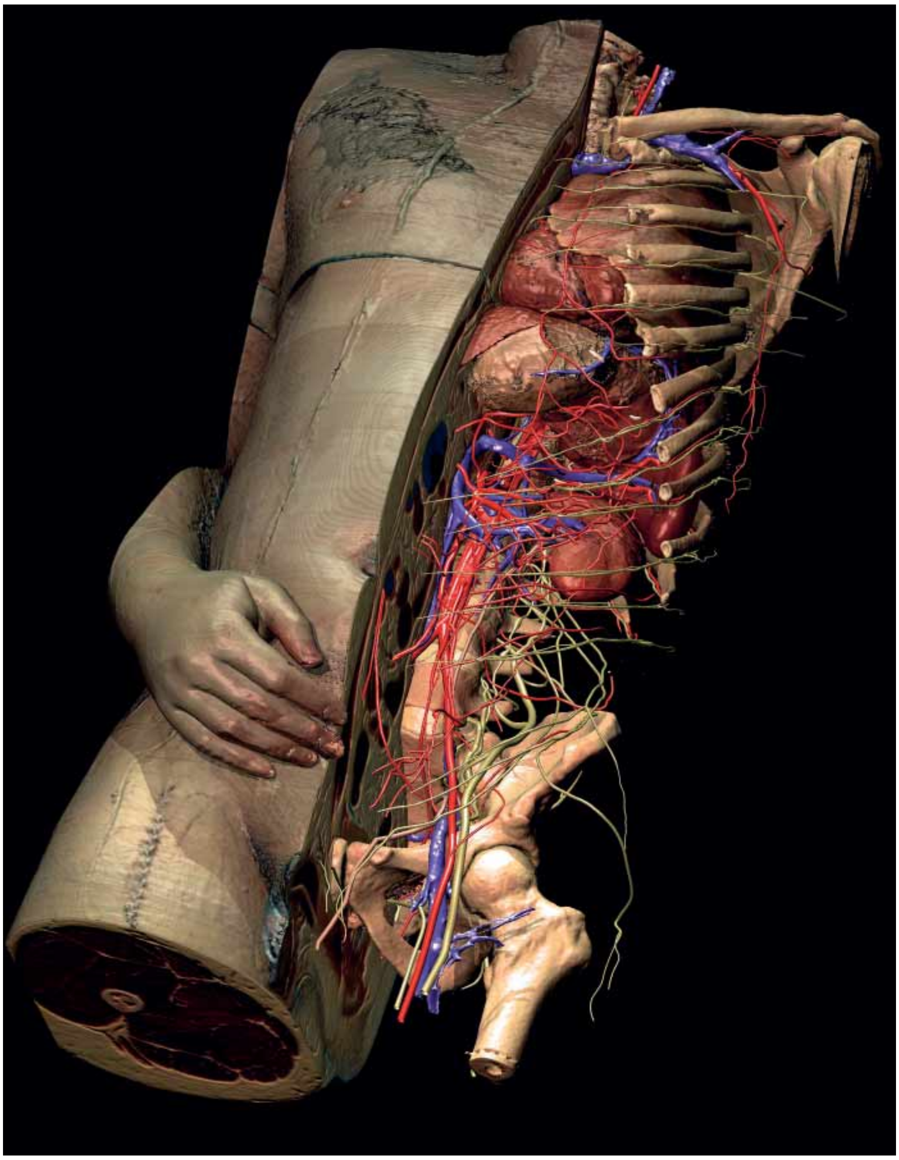

Fig. 1 3D models of inner organs in the VOXEL-MAN atlas [5] derived from the Visible Human data set. The representation exhibits a high degree of realism and detail. Yet, the model does not contain any information about inter- or intra-individual variability of human anatomy.

Most other shape descriptors like e.g. Fourier descriptors allow the establishment of correspondence on the object's surface, only.

- The model parameters invoke an intuitive understanding of an object's shape as they quantify terms like bending, thickness or elongation. This facilitates the interpretation of shape variability and allows researchers to argue about identified shape differences in anatomically meaningful terms of organ development and deformation.

2.1 Shape Representation with M-rep Models

M-reps were introduced by Pizer [21, 22] for modeling, visualization and analysis of 2D and 3D objects and are mainly used in the medical field. An m-rep model is a discrete skeletal representation of an object based on the medial axis as proposed by Blum [23]. The basic components of an m-rep model are the medial figures that have a single, non-branching medial surface and are represented as a mesh or chain of medial atoms. Simple objects like the kidney in ▶Figure 2 can be described by a single medial figure, whereas more complex objects can be built as a collection of connected figures. In this paper only one-figure objects are addressed.

The medial atoms are centers of inscribed spheres with two equal length boundary-pointing arrows that are called "spokes", at whose ends the implied boundary is to be orthogonal. A medial atom describes the local shape of the object. It is represented by the tuple $\boldsymbol{m} = (\boldsymbol{x}, r, F, \theta)$ that contains the atom's position $\boldsymbol{x} \in \mathfrak{R}^3$, the local width $r \in \mathfrak{R}^+$ (the radius of the inscribed sphere), an orthonormal local frame $F \in \mathfrak{R}^4$ that describes the object's local orientation and the object angle $\theta \in [0, \pi/2]$. The local frame $\boldsymbol{F}$ is parameterized by $(\boldsymbol{b}, \boldsymbol{b}^{\perp}, \boldsymbol{n})$, where the vector $\boldsymbol{n}$ is normal to the medial manifold and $\boldsymbol{b}$ gives the direction in the tangent plane of the fastest narrowing of the object (▶Fig. 3, left). "End atoms", i.e. atoms at the outer edge of the medial mesh, have an additional parameter $\eta \in \mathfrak{R}^+$ that describes the object's local elongation at the boundary crest (▶Fig. 3, right). The tuples $\boldsymbol{m}_i$ ($i = 1, \ldots, n$; n: number of atoms in an m-rep) for all medial atoms are combined into a feature vector that represents a given organ shape and can be used for further analysis. Further details about m-reps can be found in [22].

The medial atoms provide a figural coordinate system, giving, first a position on the medial sheet (u, v), second a figural side $t \in [-1, 1]$, and finally a relative figural distance along the appropriate medial spoke $\tau \in [-1, 0]$. Each position on the surface or in the volume of a figure, or near the figure, has assigned coordinates that describe its relative position to the medial surface which is spanned by the medial mesh. A precondition for a comparative examination of shape variants is the establishment of an appropriate geometric correspondence between objects. In the case of m-reps, the correspondence is defined on the basis of the figural coordinate system. Points on different shape variants with the same figural coordinates (u, v, t, τ) are considered to be correspondent. However, correspondence can only be defined between m-rep models that have the same topology, i.e. the same number of medial figures and the same mesh structure.

2.2 Modeling of Organ Variability

In the framework statistical models of the left kidney and of the breathing lung have been generated as examples. The kidney model is based on a population of 48 kidneys and captures inter-individual variability whereas the lung model encodes intra-individual shape variation during the breathing cycle. While the kidney model illustrates the inter-patient shape variability, the statistical model of the lung describes the intra-patient shape variability during the breathing process.

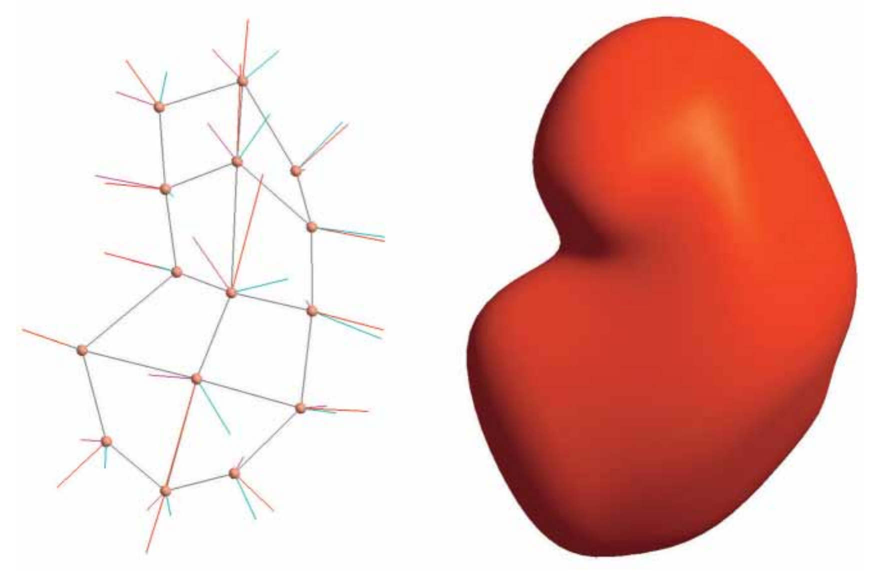

Fig. 2 An m-rep model of a kidney (left) and the implied boundary surface (right). The model is composed of a single medial figure with a mesh of 3 x 5 medial atoms. The atom's spokes are colored in turquoise and magenta.

For the kidney model we have used a population of 48 left kidneys which are based on CT data of the abdomen. An m-rep model of the kidney with a single medial figure and 3 × 5 medial atoms (►Fig. 2) was fitted to each of the segmented kidneys. For the fitting process a semiautomatic multistage optimization procedure [22] was carried out using the software "Pablo" which was developed by the Medical Image and Display Group at the University of North Carolina. During this process an objective function is minimized which optimizes the global fit of the model to the segmented image object considered and at the same time increases the likelihood of point-by-point model correspondence from one image object to the next. The global fit is measured by the mean squared distance between the model surface and the boundary of the segmented object. The correspondence is improved by favoring meshes with configurations near the starting configuration and by producing well-behaved meshes, i.e. meshes with relatively evenly spaced medial atoms. Further details of the optimization procedure are described in [22].

Employing this fitting procedure we obtained for each shape variant an m-rep model with the same medial structure and assumed point-by-point correspondence between the individual models. After aligning the models by translation and rotation an average kidney has been calculated on the basis of the m-rep parameters (►Fig. 4). During alignment of the models no scaling was done, i.e. size differences of the individual models were maintained.

Object variants can be characterized by shape and size parameters (e.g. width, bending, widening) which can be derived from the m-rep parameters. For the kidney variants we have calculated 1) the length of the medial surface as a measure of size and 2) the (global) curvature of the kidneys as a description of their shape. The length of the (curved) medial surface can be derived from the atoms' positions. The curvature is derived from the angle that is formed by the middle atom and the two related end atoms (in longitudinal direction). For the curvature the following measure is chosen: $\pi - a_i$, where a_i is the calculated angle of the kidney variant i in radians.

A standard technique for describing shape variability is principal component analysis (PCA) [24]. However, PCA is only applicable

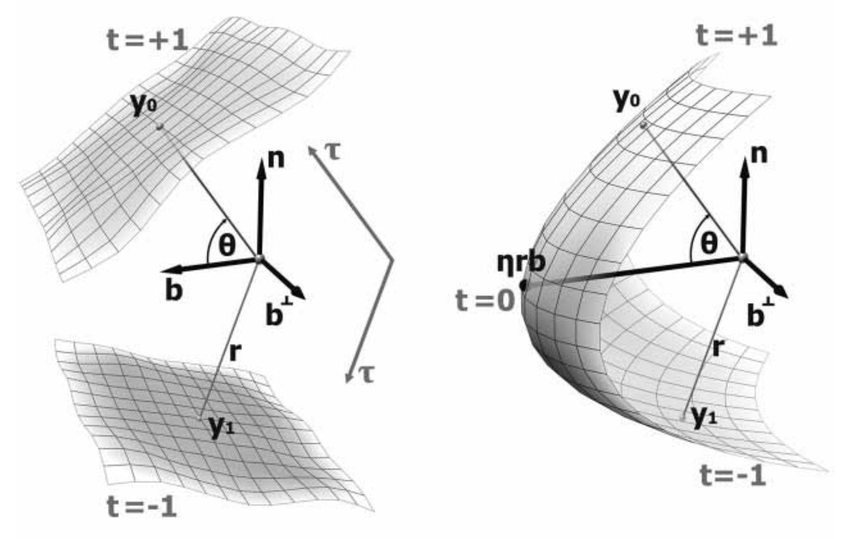

Fig. 3 Illustration of the figural coordinate system of a medial atom (left) and an end atom (right). A medial atom is represented by its position x, the length r of the two boundary-pointing arrows called "spokes", a frame made from the unit-length vector $\boldsymbol{b}$ and the two $\boldsymbol{b}$-orthogonal unit vectors $\boldsymbol{n}$ and $\boldsymbol{b}^{\perp}$, and the object angle θ between $\boldsymbol{b}$ and each spoke. The figural sides are described by t. The end atom (right), i.e. an atom at the outer edge of the medial mesh, has an additional parameter $\eta \in \Re^{+}$ that describes the object's local elongation at the boundary crest.

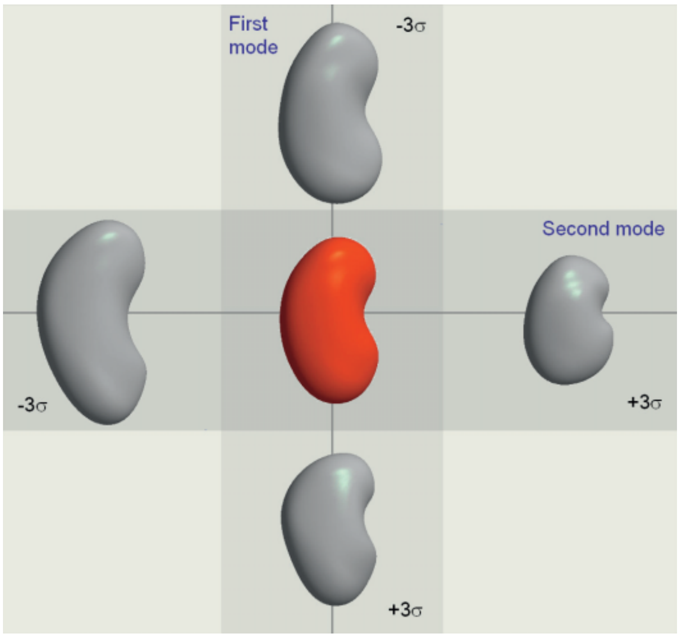

Fig. 4 The average kidney of the population (center) and the first two modes of variation in shape

for parameter vectors that are elements of the Euclidean vector space and thus can not be directly applied to m-rep models as the m-rep parameters include angles. For this reason the PCA has been extended by Fletcher et al. [25, 26] to principal geodesic analysis (PGA) which is valid for m-rep parameters. Using this method we have calculated the first principal components of the population of 48 kidneys. Figure 4 shows the mean kidney and the first and second mode of shape variation.

For integration and visualization of dynamic processes in the atlas we have also built m-rep models of the right and left lobe of the breathing lung of four patients based on 4D CT data. The 4D CT datasets were acquired in different breathing phases during free breathing. An artifact-reducing reconstruction technique [27, 28] was used to generate 3D CT data at ten points in time during the breathing cycle using optical flow-based interpolation [29].

For both the right and the left lobe of the lung we used an m-rep mesh with 6 × 7 medial atoms and fitted the m-rep models to the lung for each point in time using the described optimization procedure. ▶Figure 5 shows the m-rep model of the lung for one of the patients.

For high-quality 3D visualization of the breathing motion we interpolated the lung models in time on the basis of the m-rep parameters. That way the lung's motion during breathing can be visualized in a smooth animation. Furthermore, mean models of the breathing lung lobes as well as the first modes of their shape variations during breathing are computed using the PGA [25, 26].

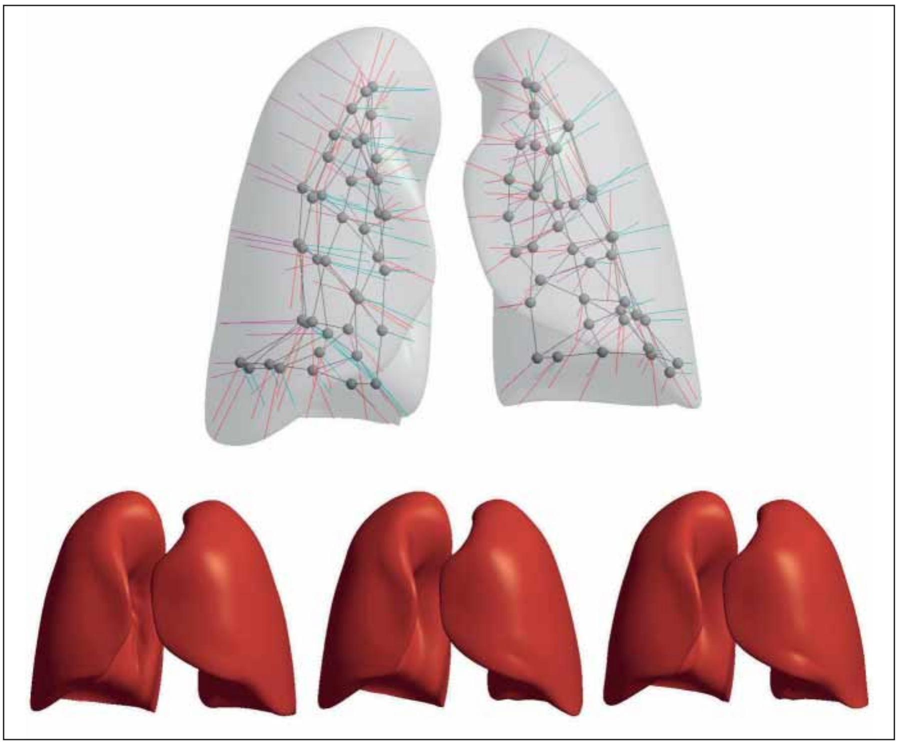

Fig. 5 An m-rep model of the breathing lung. Top: M-rep model of the right and left lobe of the lung at the time of maximum inspiration. Bottom: Surface representations of m-rep models of the lung at three points in time during the breathing cycle (left: maximum expiration; middle: mid-inspiration; right: maximum inspiration).

2.3 Integration of Shape Variability Models into the VOXEL-MAN Atlas

For the integration of a population of shape models into the VOXEL-MAN atlas two main steps are necessary. First, the shape models have to be positioned in the atlas in an anatomically sensible way, i.e. surrounding and connecting tissue and organs have to be taken into account. And second, a geometric correspondence between the shape models and the matching organ in the volume-based atlas, which we call reference organ, has to be established.

In the case of the kidney population we chose the average kidney as a representative of the population and manually fitted it to the reference kidney of the atlas using rigid transformation, i.e. size and shape of the model were conserved. The fitting was done in a way that the concave part of the kidney, i.e. the

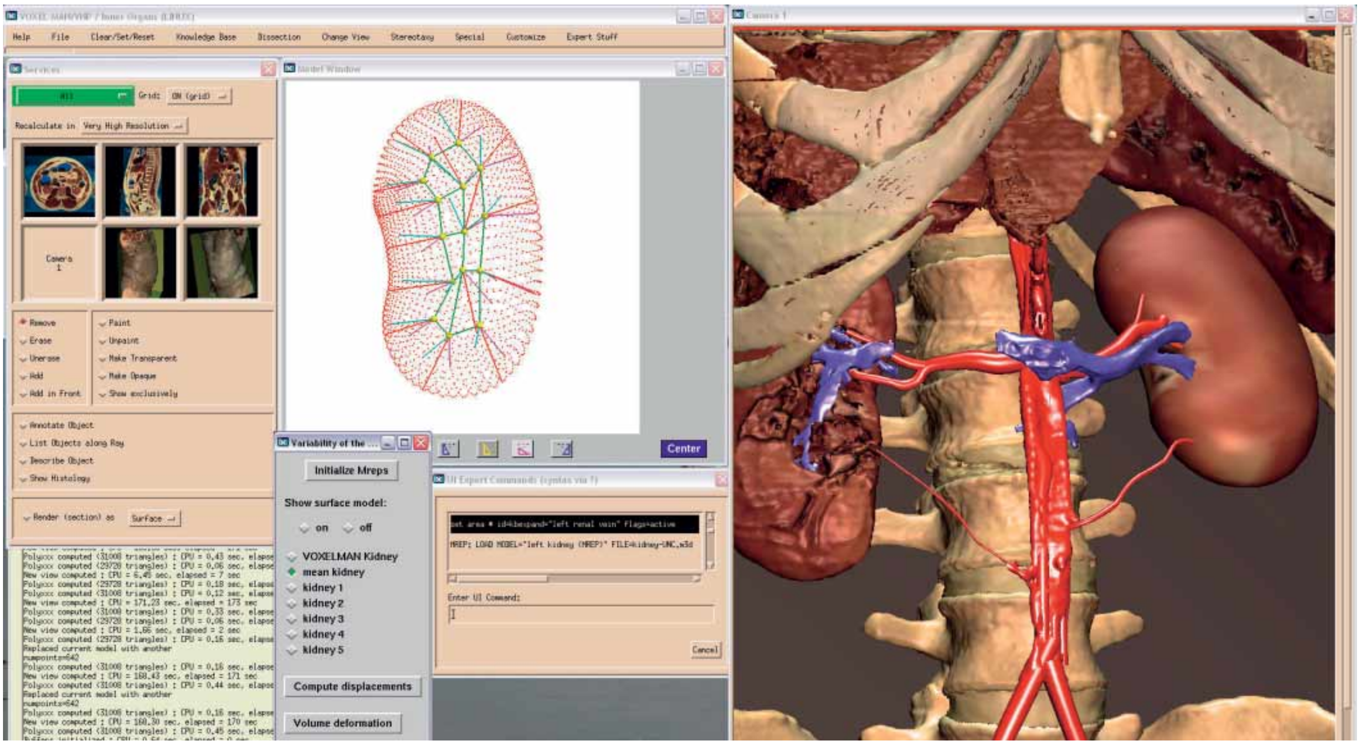

```
Polyxxx computed (31008 triangles) : CPU = 0.43 sec, elapse
Polyxxx computed (29728 triangles) : CPU = 0.06 sec, elapse
New view computed : CPU = 6.45 sec, elapsed = 7 sec
Polyxxx computed (29728 triangles) : CPU = 0.18 sec, elapse
Polyxxx computed (31008 triangles) : CPU = 0.12 sec, elapse
New view computed : CPU = 171.23 sec, elapsed = 173 sec
Polyxxx computed (31008 triangles) : CPU = 0.33 sec, elapse
Polyxxx computed (29728 triangles) : CPU = 0.06 sec, elapse
New view computed : CPU = 1.66 sec, elapsed = 2 sec
Polyxxx computed (29728 triangles) : CPU = 0.16 sec, elapse
Replaced current model with another
numpoints=642
Polyxxx computed (31008 triangles) : CPU = 0.16 sec, elapse
New view computed : CPU = 168.43 sec, elapsed = 171 sec
Polyxxx computed (31008 triangles) : CPU = 0.44 sec, elapse
Replaced current model with another
numpoints=642
Polyxxx computed (31008 triangles) : CPU = 0.16 sec, elapse
New view computed : CPU = 168.30 sec, elapsed = 170 sec
Polyxxx computed (31008 triangles) : CPU = 0.45 sec, elapse
```

```
et area * id=kbexpand="left renal vein" flags=active
MREP: LOAD MODEL="left kidney (MREP)" FILE=kidney-UNC.m3d
```

Fig. 6 User interface of the extended VOXEL-MAN system. The m-rep shape description has been integrated in the atlas and allows the exploration of shape variants of an object within the context of a volume-based 3D model. Here the mean left kidney of a population has been selected and is visualized in the scene on the right hand side. The corresponding m-rep model is shown in the window in the middle of the screen.

renal hilum, was in concordance with the atlas kidney. The renal hilum is the part where ureter and renal vein and artery are connected to the kidney and thus is an important connecting piece. For the individual kidneys that had been aligned previously the same rigid transformation was used as for the average kidney.

For the establishment of a geometric correspondence between the m-rep models and the volume-based reference kidney we fitted the average kidney model to the reference kidney of the Visible Human data by employing the optimization procedure described in Section 2.2. As a result we received an m-rep model of the Visible Human kidney which possesses the same medial structure as the other kidney models, so that a geometric correspondence between the m-reps can be defined. It serves as a reference model and represents the link between the volume-based organ of the Visible Human data and the shape variants represented by m-reps. Furthermore, it allows a deformation of the volume-based kidney according to various shape descriptions.

For the lung model a time point during the breathing cycle has been selected for which the shape of the lung was closest to the lung of the Visible Human data. As these data are derived from a dead person its lung is not in one of the natural breathing phases but in an anomalous position. The m-rep models of the right and the left lobe of the lung of the selected phase were fitted to the lobes of the Visible Human lung, so that a reference model of the lung was received. In the case of the lung we did not aim at visualizing the various lung shapes of different individuals but transferring the movement of the breathing lung to the lung of the Visible Human. For that we extracted the shape changes of the lungs between the successive points in time during the breathing cycle and applied them to the Visible Human lung.

For a surface visualization of an m-rep model the RGB values from the photographic Visible Human data set are used, giving the organs their natural colors. For a correct color mapping the geometric correspondence between the reference model and the m-rep model of interest is utilized.

To obtain a volume-based representation of a shape variant represented by an m-rep model a method has been developed that allows the deformation of the volumetric model of the organ in the Visible Human data set according to the m-rep coordinates. By this transformation internal structures of the reference kidney are deformed to visualize internal structures in the m-rep models of the population. The transformation field for this deformation is determined as follows:

First, for each voxel (x, y, z) belonging to the reference organ in the atlas the figural coordinates (u, v, t, τ) are calculated using the reference m-rep model of the organ. Then, the figural coordinates received are transferred to the m-rep model of the considered shape variant and its position in the atlas coordinate system is determined.

After calculation of the transformation field the deformed volume has to be generated. For doing this a transition from the continuous coordinates of the transformation field to the discrete voxel coordinates of the target image is necessary which is done by a procedure called resampling. An overview of resampling methods used in the field of image processing is given in [27]. We have employed an inverse method, i.e. for each voxel in the target volume a transformation vector is calculated. For calculation of the RGB values in the target volume we have used tri-linear interpolation which results in a certain smoothing effect but has been shown to be sufficient for our visualization purposes.

For a reconstruction of the deformed object's surface with subvoxel resolution the described transformation is calculated not only for voxels belonging to the considered object but also for a layer of voxels surrounding the object.

The transformation developed enables the visualization of surface and internal structures in high quality.

3. Results

With the integration of m-rep-based shape descriptions into the VOXEL-MAN atlas it is now possible to query and visualize different shape variations of an organ within the context of a volume-based anatomical model (▶Fig. 6). Attributes like gender, age or pathology can be assigned to each shape variant which then can be visualized by specifying these attributes. In addition to the representation of inter-individual shape variations (▶Fig. 7) or the average shape of a population (Fig. 6), intra-individual shape variations can be visualized as well, in our example lung motion induced by breathing.

Shape variants can also be visualized according to shape and size parameters that have previously been derived from the m-rep parameters and they can be arranged in a sorted sequence. ▶Figure 8 shows an example in which the kidney variants are sorted by length of the medial surface and by curvature. The organs could also be arranged according to other attributes, like e.g. the patient's age. That way it would be possible to visualize age-specific differences of an organ that appear in different periods of life (e.g. infancy, youth, maturity, age).

For illustration of variability in shape within a population the principal components received from PGA are utilized (see Section 2.2). The organ shape can be visualized while moving along the first or second principal axes which are the axes in shape space in direction of the greatest variance (▶Fig. 4). That way an impression of the most prevalent variations in shape within a population can be seen.

The shape variants may be depicted as surface models which can be rapidly calculated from the m-rep models. In this way a quick overview can be gained about the shape variability of a population of organs. The surface models are visualized in the organs' natural colors giving them a more realistic look (▶Fig. 7). However, as the surface colors were derived from the Visible Human data set, they do not reflect the original colors of the individual shape variants.

Besides a surface representation, a volume-based representation of an organ's shape variants can also be generated. It results from the deformation of the reference organ of the volume-based model according to the m-rep shape description. This way a realistic visualization of the shape variants is possible, as well as the visualization of the organ's internal structures. As an example a kidney variant is shown after the application of cutting operations (▶Fig. 9).

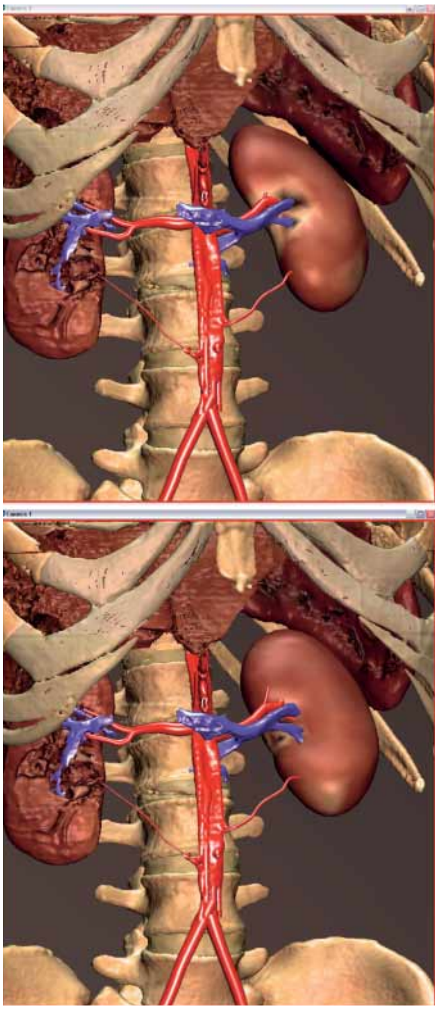

Fig. 7 Visualization of shape variants of the kidney within the VOXEL-MAN atlas. The left kidneys (in the pictures on the right hand side) are surface representations on the basis of m-rep models. Top: left kidney of the Visible Human. Bottom: a shape variant of the kidney selected out of 48 shape models available.

4. Discussion

The inclusion of anatomical variability in a 3D interactive atlas presents considerable challenges, since such a system must capture how anatomic structures vary in large populations, across age, gender and races, and in different disease states. We have presented a new approach for a variability atlas that is based on the VOXEL-MAN atlas and extends it by the m-rep shape description for modeling variability of anatomical objects. With the connection of a volume-based atlas and skeleton-based shape description the advantages of both methods are combined. The key advantages of the system presented are as follows:

- A volume-based model allows a highly realistic representation of the anatomy. In the VOXEL-MAN atlas anatomical structures are reconstructed with subvoxel resolution and are visualized using their natural colors. The result is a visual impression with high realism.
- The VOXEL-MAN atlas is a highly flexible tool for exploring the human anatomy. The integrated knowledge base allows a versatile interaction with the spatial model, e.g. the anatomical model can be interrogated or disassembled. Also, the model can be rotated in all directions and cutting planes can be placed and the interior of anatomical structures can be viewed, and so on. The whole functionality of the atlas is also accessible in the extended version presented.
- The m-rep shape description allows a compact representation of shape variability, i.e. characteristic shape properties are represented with a restricted number of parameters (in contrast e.g. to deformation fields). For a variability atlas that is designed for representing a high number of shape variants, a compact shape de-

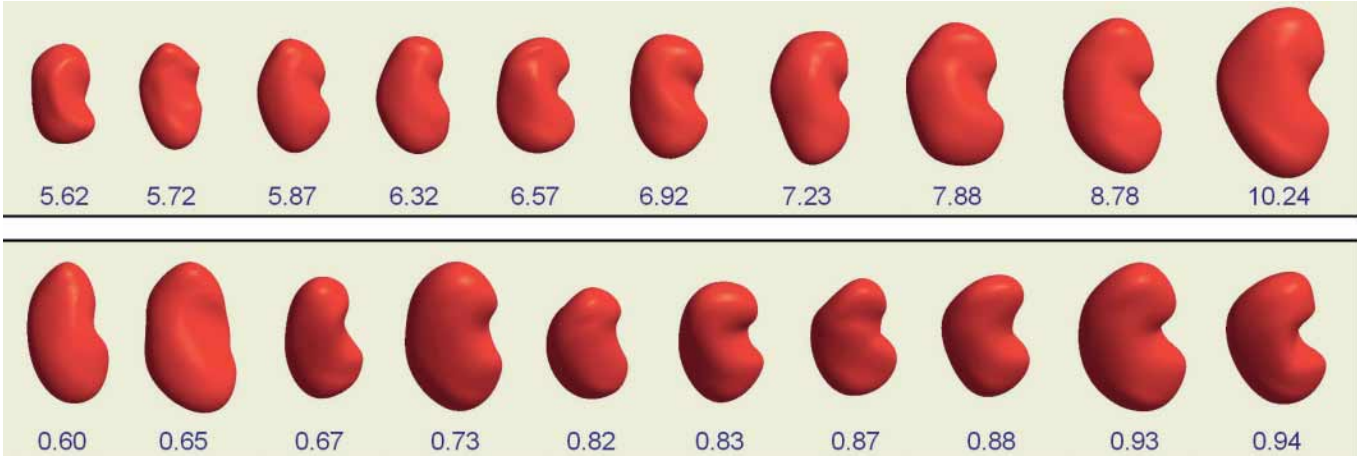

Fig. 8 Shape variants can be characterized by shape and size parameters and arranged in a sorted sequence. Top: kidney variants sorted by length of medial surface (in cm). Bottom: kidney variants sorted by curvature ($\pi - a_i$, where a_i is the angle of variant i in radians).

scription is a prerequisite if the system should be able to run on standard PCs.

We demonstrated the concept and functionality of this atlas using a statistical shape model of the kidney and a model of the breathing lung as examples. With the integration of the m-rep shape description into the VOXEL-MAN atlas it is now possible to query and visualize different shape variations of an organ, the average shape and main modes of variation in a population.

Yet the approach presented has also its restrictions and limitations. One major issue is the interdependency of neighboring organs or structures regarding their shape and position. If the shape of an organ changes the surrounding structures naturally also move or deform which haven't been taken into account so far in the system presented. In our examples we have used only m-rep models consisting of a single object (the kidney) or two objects (lobes of the lung). For modeling the dependency of neighboring organs it is necessary to build m-rep models for all organs of interest and combine them in a group.

Another restriction is that visualizations of all shape variants are based on the same photographic data set. For both the surface-based and the volume-based visualizations of shape variants the RGB values of the corresponding organ in the Visible Human data set are used and thus they do not reflect individual differences in color of these variants. While the visualization of shape variants in their original colors is a desirable goal it didn't seem to be a realistic one for two reasons.

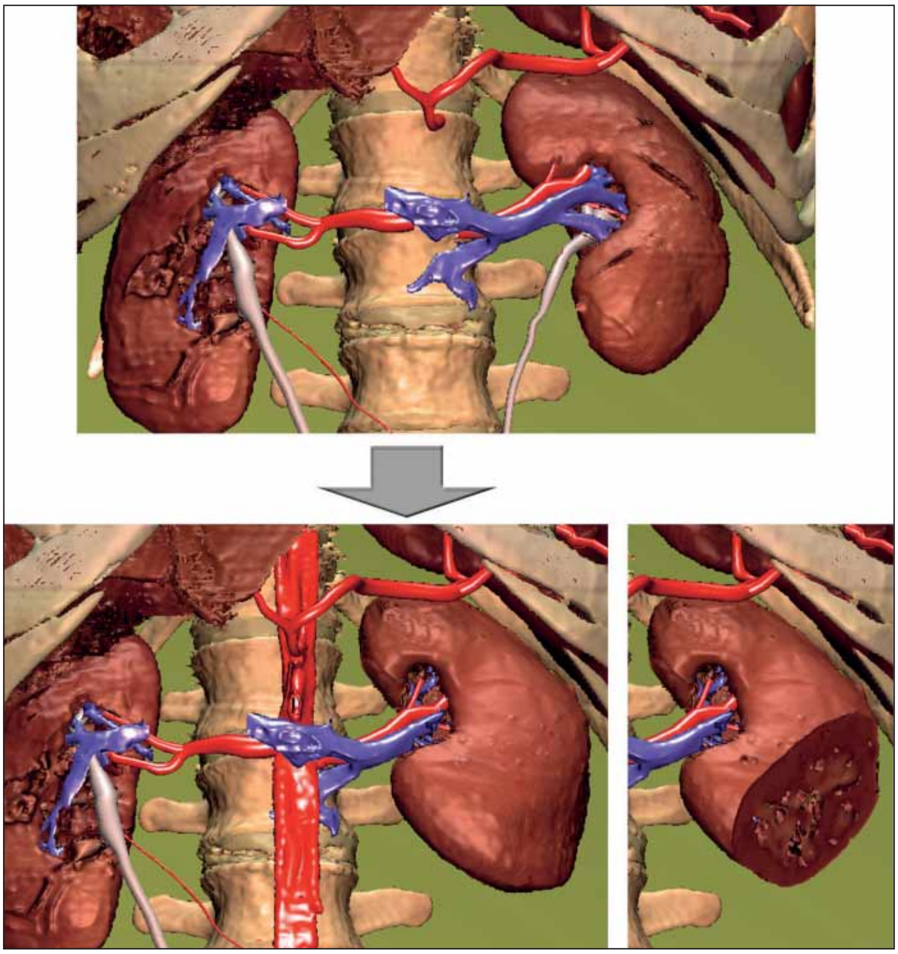

Fig. 9 Volume-based representation of shape variants of the left kidney in the VOXEL-MAN atlas. Top: reference kidney from the original volume model (Visible Human). Bottom: volume representation of a shape variant of a kidney based on an m-rep description. The cut-away gives an insight to the interior of the kidney.

First, photographic volume data are only available for a very limited number of subjects and naturally not for patients. And second, storing photographic data for each shape variant would result in a huge amount of data – which is what we wanted to avoid by choosing a compact shape description.

Also, it should be obvious that the approach presented is not reasonable for pathological variants that show substantial morphological differences to a healthy kidney. However, all healthy and pathological structures and organs with similar shape can be represented in the atlas by this technique.

5. Conclusion

We developed a framework for representation and visualization of shape variability within a 3D interactive anatomical atlas using an organ-based approach. It could be a basis for the development of specialized variability atlases that focus e.g. on specific regions of the human body, groups of organs or specific topics of interest. If filled with appropriate data such an atlas might be able to answer questions like the following:

- What range of variations of organs is considered "normal"?
- What are the effects of disease on shape and size of anatomical structures?
- How do organs change during growth and under normal ageing?
- How is the shape of an anatomical structure related to factors like gender, habits or environmental influences?

Possible applications of such variability atlases are mainly in the area of medical education but they could e.g. also serve as reference for health professionals. However, currently the use of statistical shape models in anatomical atlases is still in its infancy and there are only limited experiences available with the use of such statistical shape information in medical education. We have used our atlases of the kidney and the lung in seminars with medical students of the University Medical Center Hamburg-Eppendorf to show the range of possibilities of statistical anatomical atlases. The response was very positive, however a more detailed and extended evaluation of the educational benefits of the atlas showing shape variations of organs should be performed.

In the current state of implementation, the Visible Human data set is used as reference data set in the extended VOXEL-MAN atlas. In principle, it is also possible to use other data sets, e.g. CT or MRI data sets, as reference data set in the framework. However, in CT or MRI data sets it is harder to segment fine anatomical structures because of the reduced image resolution and contrast in comparison to the high-resolution colored Visible Human data set. Hence, it is expected that the number of segmented structures represented in such an atlas will be strongly reduced in comparison to our currently available reference atlas. Furthermore, a complete segmentation of all relevant structures has to be performed to generate a new reference atlas and an adapted knowledge base has to be created. Hence, the effort to generate another reference data set is very high.

The presented framework for representation and visualization of 3D shape variability of organs opens up new insights into the intra- and inter-individual shape variety of organs in an interactive 3D atlas. Further discussions with medical experts are needed to identify medical disciplines and applications where this new kind of information is helpful. Especially, it has to be explored how useful visualizations of statistical anatomical variants in an atlas environment are beyond the educational setting, e.g. in clinical applications and studies.

Acknowledgments

We thank Stephen Pizer and the image processing group (MIDAG) of UNC in Chapel Hill for the provision of the software "Pablo" and the support in all problems and questions regarding the m-reps. We are also grateful to the members of the radiation oncology at UNC for providing the kidney data. We thank Karl-Heinz Höhne for the possibility to extend the VOXEL-MAN atlas in this project. This work is supported by the German Research Foundation (DFG).

References

1. Ackerman MJ. The Visible Human Project: A Resource for Anatomical Visualization. Medinfo 1998. pp 1030–1032.
2. Spitzer V, Ackerman M, Scherzinger A, Withlock D. The Visible Human Male: A Technical Report. J Am Med Inform Assoc 1996; 3 (2): 118–130.
3. Zhang SX, Heng PA, Liu ZJ, Tan LW, Qiu MG, Li QY, Liao RX, Li K, Cui GY, Guo YL, Yang XP, Liu GJ, Shan JL, Liu JJ, Zhang WG, Chen XH, Chen JH, Wang J, Chen W, Lu M, You J, Pang XL, Xiao H, Xie YM, Chun-Yiu Cheng J. The Chinese Visible Human (CVH) Datasets Incorporate Technical and Imaging Advances on Earlier Digital Humans. J Anat 2004; 204: 165–173.
4. Riemer M, Park JS, Chung MS, Handels H. Improving the 3D Visualization of the Visible Korean Human via Data Driven 3D Segmentation in RGB Color Space. World Congress on Medical Physics and Biomedical Engineering 2006, 14 (31). Springer, 2007. pp 4200–4203.
5. Höhne KH, Pflesser B, Pommert A, Riemer M, Schubert R, Schiemann T, Tiede U, Schumacher U. A Realistic Model of Human Structure from the Visible Human Data. Methods Inf Med 2001; 40: 83–89.
6. Structural Informatics Group. Interactive Atlases: Digital Anatomist Project. Dept. of Biological Structure, University of Washington, Seattle, WA, 2004. http://www9.biostr.washington.edu/da.html.
7. Bergman RA, Adel K, Miyauchi R. Illustrated Encyclopedia of Human Anatomic Variation. University of Iowa, 2004. http://www.anatomyatlases.org/AnatomicVariants/AnatomyHP.shtml.
8. Toga AW, Thompson PM. Multimodal Brain Atlases. In: Wong S (ed.). Advances in Biomedical Image Databases. New York: Academic Press; 1999.
9. Mazziotta JC. A Probabilistic Atlas and Reference System for the Human Brain. In: Toga RW, Mazziotta JC. Brain Mapping – The Methods. San Diego: Academic Press; 2002. pp 727–755.
10. Thompson PM, Mega MS, Woods R, Zoumalan CI, Lindshield CJ, Blanton RE, Moussai J, Holmes CJ, Cummings JL, Toga AW. Cortical Change in Alzheimer's Disease Detected with a Disease-specific Population-based Brain Atlas. Cereb Cortex 2001; 11 (1): 1–16.
11. Bailleul J, Ruan S, Bloyet D. Automatic atlas-based Building of Point Distribution Model for Segmentation of Anatomical Structures from Brain MRI. Proc Signal Processing and its Applications 2003; 2: 629–630.
12. Joshi S, Pizer SM, Fletcher PT, Yushkevich P, Thall A, Marron JS. Multiscale Deformable Model Segmentation and Statistical Shape Analysis using Medial Descriptions. IEEE Trans Med Imaging 2002; 21: 538–550.
13. Golland P, Grimson WEL, Kikinis R. Statistical Shape Analysis Using Fixed Topology Skeletons: Corpus Callosum Study. Information Processing in Medical Imaging (IPMI) 1999. pp 382–387.
14. Staib L, Duncan J. Boundary Finding with Parametrically Models. IEEE PAMI 1992; 14 (11): 1061–1075.
15. Kelemen A, Szekely G, Gerig G. Elastic Model-Based Segmentation of 3D Neurological Data Sets. IEEE Trans Med Imaging 1999; 18: 828–839.
16. Styner M, Gerig G. Hybrid Boundary-medial Shape Description for Biologically Variable Shapes. Proc IEEE Workshop on Mathematical Methods in Biomedical Image Analysis (MMBIA) 2000. pp 235–242.
17. Cootes TF, Taylor CJ. Active Shape Models – "Smart Snakes". In: Hogg et al. (eds.). BMVC92. Proceedings of the British Machine Vision Conference. Berlin: Springer-Verlag; 1992. pp 266–275.

18. Tiede U, Schiemann T, Höhne KH. High Quality Rendering of Attributed Volume Data. In: Ebert D, Hagen H, Rushmeier H (eds.). Proc. IEEE Visualization 1998. Research Triangle Park, NC; 1998. pp 255–262.
19. Pommert A, Schubert R, Riemer M, Schiemann T, Höhne KH. Symbolic Modeling of Human Anatomy for Visualization and Simulation. In: Robb RA (ed.). Visualization in Biomedical Computing 1994. Rochester; 1994. pp 412–423.
20. Höhne KH, Pflesser B, Pommert A, Riemer M, Schubert R, Tiede U. A New Representation of Knowledge Concerning Human Anatomy and Function. Nature Med 1995; 1 (6): 506–511.
21. Pizer SM, Fritsch D, Yushkevich P, Johnson V, Chaney E. Segmentation, Registration, and Measurement of Shape Variation via Image Object Shape. IEEE Trans Med Imaging 1999; 18: 851–865.
22. Pizer SM, Fletcher PT, Joshi SC, Stough J, Thall A, Chen JZ, Fridman Y, Fritsch DS, Gash G, Glotzer JM, Jiroutek MR, Lu C, Muller KE, Tracton G, Yushkevich PA, Chaney E L. Deformable M-reps for 3D Medical Image Segmentation. Int J Comp Vis 2003; 55: 85–106.
23. Blum TO. A Transformation for Extracting New Descriptors of Shape. In: Wathen-Dunn (ed.). Models for the Perception of Speech and Visual Form. Cambridge, MA: MIT Press; 1967. pp 362–380.
24. Jollife IT. Principal Component Analysis. Springer-Verlag; 1986.
25. Fletcher PT, Lu C, Joshi S. Statistics of Shape via Principal Component Analysis on Lie Groups. IEEE Computer Society Conference on Computer Vision and Pattern Recognition (CVPR) 2003. pp 95–101.
26. Fletcher PT, Joshi S, Lu C Pizer SM. Gaussian Distribution on Lie Groups and their Application to Statistical Shape Analysis. In: Taylor C, Noble JA (eds.), Information Processing in Medical Imaging (IPMI) 2003. pp 450–462.
27. Ehrhardt J, Werner R, Frenzel T, Säring D, Lu W, Low D, Handels H. Optical Flow based Method for Improved Reconstruction of 4D CT Data Sets Acquired During Free Breathing. Med Phys 2007; 34 (2): 711–721.
28. Werner R, Ehrhardt J, Frenzel T, Säring D, Lu W, Low D, Handels H. Motion Artifact Reducing Reconstruction of 4D CT Image Data for the Analysis of Respiratory Dynamics. Methods Inf Med 2007; 46: 254–260.
29. Ehrhardt J, Säring D, Handels H. Structure-preserving Interpolation of Temporal and Spatial Image Sequences using an Optical Flow-based Method. Methods Inf Med 2007; 46: 300–307.